ALUMINIUM MASTER ALLOYS WITH REDUCED INTERMETALLIC PHASE SIZES OPEN UP WINDOWS FOR NEW APPLICATIONS

M. Vader, J. Noordegraaf and P.C. van Wiggen
Kawecki-Billiton Metaalindustrie B.V.
Kloosterlaan 2, 9936 TE Delfzijl, The Netherlands

Abstract

Intermetallic phase control and rapid cooling are the basis of the production process for the new generation of sophisticated master alloys.
Ductile fast dissolving products with intermetallic particles of less than 5µm. offer an excellent means for enhanced in-line treatment.
Grain refining, modification and alloying all benefit from the remarkable advantages of phase control.

Introduction

It has been a long standing ambition to predict the dissolution time of a master alloy. A study, attempting to provide a more scientific basis for the dissolution of phases, has shown that a literature model can be adapted to all dissolving phases in liquid aluminium.
In addition, the know-how generated through this model enables the prediction of the performance of existing and new products.
This model will be applied to three areas related to the dissolution of:

- Phases in AlTiB grain refiners;
- Mn and Fe carriers;
- Modifiers and other master alloys.

The model for dissolution rates:

Studies performed by O'Malley (ref. 1) et al, Paret and d'Hondt (ref. 2), have shown that the dissolution rate of Manganese metal can be predicted, to a large extent, by taking into account the rather complex function of melt composition, particle size and some physical properties.
It was demonstrated that the dissolution rate of Mn carriers depends on the linearity of both the density of the Manganese containing phase and the size of this phase.

This model was also applied to other binary alloys and the predicted dissolution rates corresponded very well with practical experience.
The dissolution time is dependent on the following parameters, keeping in mind that the latter two are determined by the actual melt temperature:

- particle size
- particle density
- initial and final composition
- equilibrium conditions determined by the phase diagrams

The two mechanisms of fluid flow and rate of diffusion are combined in this simplified model. We find that the great advantage of the model is that it corresponds so well with practice.
The model was converted to SI-units and is included as Appendix I.
The solution time for typical master alloys in Al has been calculated with these equations and results are illustrated in Table I.

Master alloys	(Inter)-metallic phase density $10^3 kg/m^3$	Diameter (mm)	Aim concentration %	Dissolution time min.		Remarks (Al_3Ti thickness) µm
				700°C	750°C	
AlTi	3.15	0.2	0.2	78	30	200
AlTi	3.15	0.02	0.2	7.4	3	20
AlTi	3.15	0.04	0.002	6.0	3.6	40
AlTi	3.15	0.04	0.2	15.5	6.3	40
AlTi	3.15	0.01	0.01	1.57	1.0	10
AlTiB5/1	3.15	0.01	0.01	1.57	1.0	10
AlFe45 splatter	4.0	1.0 #	1.0	30	13	
Mn Powder	7.43	1.5	1.0	51	22	
Mn AlloyPack	7.43	0.25	1.0	8	4	
AlMn60 splatter	4.5	1.0 #	1.0	20	9	
AlCr20	3.26	0.3	0.2	16.7	8.5	
AlCu50	5.9	<0.1	1.0	1.5	1.2	
AlNi20	4.25	0.1	0.2	0.5	0.4	
AlSi50	2.33	0.2	0.1	0.3	0.24	
AlSr 10	2.6	0.2	0.05	1.12	0.75	
AlSr 10 *	2.6	0.005	0.05	2 sec	1 sec	
AlZr	3.65	0.2	0.2	57	20	
AlB	2.3	0.004	0.004	0.72	–	5µm AlB_2
# particles obtained due to the shattering effect of splatter * fine phased, employing KBM's patented production process						

Table 1: Dissolution time for typical master alloys in Aluminium.

Implication for grain refinement:

The solidification of a melt is influenced by the addition of an AlTiB grain refiner, through which TiB_2 and Al_3Ti are added to the melt. The dissolution of the two phases plays a crucial role in the mechanism of grain refinement. With regard to the developed model, the rate of dissolution of TiB_2 and Al_3Ti was calculated. In addition, the stability of TiB_2 as a function of the % Ti and % B in the AlTiB alloys was determined. As a result of the data obtained, additional information has been gained regarding the mechanism of grain refinement,

The grain refining mechanism and, in particular, the role of the aluminide has been a subject of study for the past 70 years. As early as 1923, Van Erckelens (see ref. 3) reported effects resulting from the addition of Titanium in Aluminium. In his work he described the Al_4Ti phase, which nowadays has been better qualified as Al_3Ti.

For a number of years now, the grain refining mechanism has been the subject of a research project carried out by:

Stockholm University on behalf of Kawecki-Billiton Master Alloys.

The peritectic "Hulk" theory, first presented at the TMS Annual General Meeting in 1989 (ref. 4), has been further substantiated. During the 1990 TMS Meeting (ref. 5), the nucleation and growth phenomena were modelled and supported by experiments carried out by Stockholm University (ref. 6 and 7). The rate determining steps were studied in depth and a series of 10 steps were proposed in the mechanism leading to the formation and subsequent activation of growth centers. These 10 steps are simmarized below:

The mechanism, as previously reported, comprises of several sequential stages.

* melting of the grain refiner into the Aluminium
* dissolution of TiB_2 and Al_3Ti
* diffusion of Ti and B into the melt
* coverage of Al_3Ti particles
* completion of the peritectic cell
* evaluation of the peritectic "Hulk"
* formation of a peritectic liquid inside the shell
* nucleation of α-Aluminium
* growth of α-Aluminium
* completion of the solidified product.

The steps concerning dissolution, diffusion and coverage will be discussed in more detail, as will implications for the formation of the encapsulating layer around an aluminide.

The rate of dissolution for Al_3Ti:

The Al_3Ti dissolution rate can be calculated depending the addition and the particle size of AlTiB. In figure 1, the relation between aimed Ti and time for the different $TiAl_3$ particle sizes is plotted.

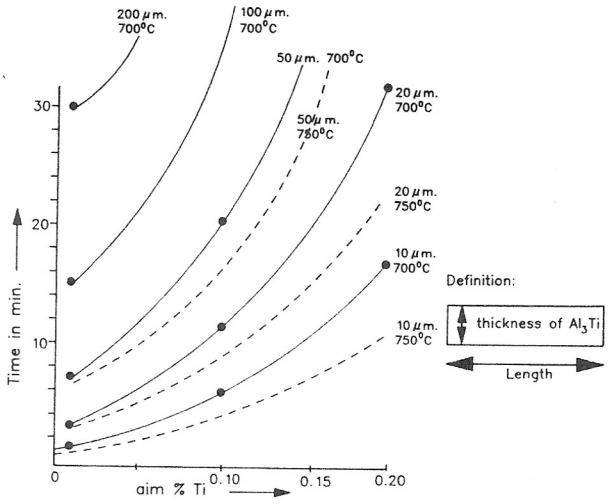

Figure 1: Calculated dissolution time of Al_3Ti particles as a function of thickness, temperature and aim concentration.

The rate of dissolution for TiB_2:

The calculation is based on Finch's solubility data (see ref. 8). This is illustrated in Table II.

AlTiB(5/1) kg/ton	Addition		Solubility # at 750 °C
	ppm Ti	ppm B	ppm B
2	100	20	0.5
1	50	10	0.69
0.5	25	5	0.97
0.2	10	2	1.5
0.1	5	1	>1
# %Ti is considered fixed at added quantity			

Table II: Solubility of B as a function of Ti-content.

An addition of a given quantity of AlTiB (in kg/ton) corresponds to an added % Ti (see Table II). This % Ti determines the solubility of % B. If the % Ti is reduced, solubility of B is increased, as

$(\%Ti).(\%B)^2$ = constant.

It can be understood from the aforementioned data that the size of the Al_3Ti phase and the value of the target concentration are very important and determine the time required for full dissolution.
When added as TiB5/1, the dissolution time for TiB_2 particles (1µm. particle size) is 2000 minutes.

$$t_{sec} = \frac{4500 \times 1.10^{-6} \times 4.8}{60 \times 3.10^{-5} \times 1.10^{-4}_{\%}} = 2000 \text{ minutes} = 1.4 \text{ days!}$$

For an 0.1µm. particle, the dissolution process would still take 3.3 hours.
In another application the quantity of TiB_2 dissolved within 2 minutes can be calculated (a standard contact time). It can be calculated that only $4.8\ 10^{-3}$ ppm B can become dissolved at a temperature of 750°C. within 2 minutes.
Boron will not, therefore, reduce the Al_3Ti dissolution rate by a reduction of the Ti solubility. Instead, the dissolution rate of Al_3Ti determines the dissolution rate of TiB_2.
Assuming a 500µm. grain size in the final product and also assuming a 5µm. Al_3Ti "Hulk" size, one can calculate the amount of TiB_2 needed to cover the Al_3Ti with one monolayer of TiB_2. A monolayer equals $1.4\ 10^{-6}$ kg. B/m^3 Al, divided by 2700 (kg/m^3) which yields as little as $5.2\ 10^{-4}$ ppm B, considerably less than the $4.8\ 10^{-3}$ ppm dissolved in 2 min.
In conclusion it can be said that there is enough TiB_2 dissolved to allow a reprecipitation around TiB_2 of several monolayers. This indicated that the stability of the peritectic "Hulk" comprises a true equilibrium.

Stability of TiB_2:

Using Finch's data the stability of TiB_2 at four different temperatures, viz. 750, 725, 700 and 675°C., was calculated. It appears that the highest stability of TiB_2 is realized with the 5/1 ratio, the optimal ratio being the 4,5:1 ratio. Figure 2 depicts the stability of TiB_2 as a function of addition (kg/ton) and the Ti/B ratio in the AlTiB grain refiner.
The statistical variations in the chemical composition, e.g. 4.5-5.5% Ti and 0.15 - 0.25 % B for the 5/0.2 ratio, give a variation around the nominal ratio.
It appears that this does not apply to the AlTiB5/1 (see figure 2.). With a lower B content however, the variation may be such that stability of TiB_2 is only maintained at a relatively high addition (kg/ton). The variations that may occur due to the inherent alloy chemistry are plotted in figure 2 around the nominal value of the Ti/B ratio.

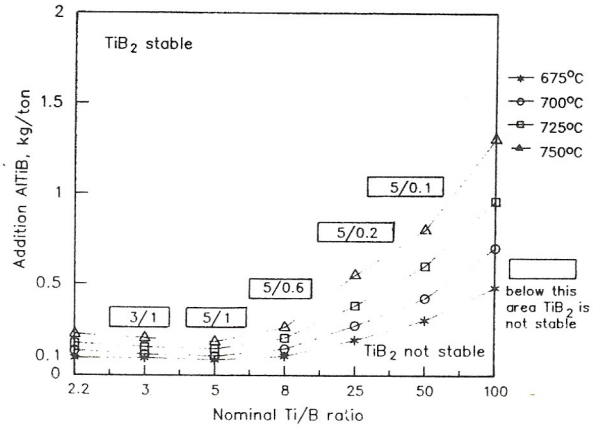

Figure 2: TiB_2 stability for some Ti/B ratio's.

With the most ideal situation (ultra-fine and homogeneously distributed Al_3Ti and TiB_2) equilibrium conditions can be achieved immediately. Because commercial grain refiners can not as yet attain this ideal situation, a two times higher doses has to be added to guarantee the survival of stable TiB_2 particles. This leads to the following table (Table III), in which both the theoretical and practical lowest addition rate is plotted.

Master Alloys	Theoretical limit	Practical limit
5/1	0.2	0.4
3/1	0.25	0.5
5/0.6	0.4	0.8
5/0.2	0.7	1.4
5/0.1	1.0	2.0
5/0.05	1.4	2.8
5/0.025	±2.0	±4.0

Table III: Theoretical and practical addition rate.

It can be concluded that TiB_2 will always dissolve at a very low rate. The curves of figure 2 determine under which conditions reprecipitation of TiB_2 may take place. These curves were calculated using the Finch solubility data.
If TiB_2 is not stable, the added TiB_2 will dissolve and only local reprecipitation of TiB_2 on dissolving Al_3Ti species may still take place. Immediately after the formation of a shell the TiB_2, due to its large specific surface, will dissolve again.

In principle, this will occur faster when compared with 1µm. TiB_2 particles already present. The reprecipitated TiB_2 will only be able to protect a "Hulk" if the TiB_2 is stable.
The casting temperature appears to be critical for low Boron master alloys. Even 5/0.2 may be expected to suffer from a too high casting temperature.
In view of this, the development of a low Boron AlTiB alloy should aim at Boron content in excess of 0.05%B, preferably 0.1-0.2% B. Along similar lines, the development of an AlTiC alloy limits the useful carbon content.
It is clear that the most efficient grain refiners should contain both small TiB_2 particles and Al_3Ti particles. It can now be understood why the 5/1 ratio yields the best grain refinement (see ref. 10) which can be traced back to the solubility product of TiB_2.

Implication for Mn and Fe carriers:

A typical example of a fine phased, rapidly cooled master alloy is the in Europe widely used splatter Aluminium which consists of 60% Manganese or 45% Iron.

1. Splatter is a true intermetallic phase. The elements undergo a high temperature reaction in liquid state before rapid solidification by splat casting to retain the single intermetallic phase. The final product consists of individual pieces of randomly shaped flakes with an average thickness of between 1 and 4mm., offering a considerable surface to volume ratio.

2. This alloy with a large surface area guarantees a relatively short dissolution time. A phenomenon that enhances dissolution is the shattering effect. Upon addition to the melt, internal stresses cause the splatter to disintegrate. This type of structure fragments rapidly dissolve in Aluminium. An additional advantage is that the master alloy is a full metals product generating a minimal dross yield.

The characteristics of the most commonly used Mn and Fe carriers are listed in Table IV. Both the phases present and the % of Mn or Fe are indicated.

Mn carrier	Nominal % Mn	Metallurgical phases present	Shape of Mn contained in carrier
Mn flakes	100	Metallic Mn	flakes
Mn powder injection quality	100	Metallic Mn	powder
AlMn10 ingot	10	Al_6Mn intermetallic in Al matrix	needle
AlMn60 splatter	60	Al_8Mn_5 intermetallic	flakes
AlMn75 compacts	75	Metallic Mn + Al foil powder	powder
Mn75 flux tablets	75	Metallic Mn + flux + Al foil powder	powder
Mn80 AlloyPack	80	powder + flux	powder

Fe carrier	Nominal % Mn	Metallurgical phases present	Shape of Fe contained in carrier
AlFe10 ingot	10	Al_3Fe in Al matrix	needles
AlFe25 ingot	25	Al_3Fe in Al matrix	needles
AlFe45 splatter	45	Al_9Fe_2 intermetallic	flak s
Fe75 flux tablets	75	Metallic Fe flux + Al foil powder	powder
AlFe75 compacts	75	Metallic Fe + Al foil	powder
Fe80 AlloyPack	80	Powder + flux	powder

Table IV: Characterization of commonly used Mn and Iron carriers.

In addition to phase size and scatting, parameters such as wetting and dispersion should be taken into account to predict the rate of dissolution.
Wetting can be described as the ability of an alloying constituent to make intimate contact with liquid Aluminium in order to enable the transfer of atoms from the carrier to the melt. A master alloy with an Al-Mn intermetallic contained in an Al matrix best fulfills this requirement. This is, in principle, the case with AlMn10 waffle plate and AlMn60 splatter. All the other Mn carriers contain metallic Mn powder with a size ranging from 4 to 0.2mm.

Dispersion and stirring:

An additional requirement for dissolution is that the carrier be properly dispersed throughout the batch, followed by controlled mechanical stirring or by gentle gas bubbling.

Dross formation:

The Aluminium and flux contained in the powder/ mixtures will generate some residual phases. The flux will be lost completely and will show up in the dross. The Aluminium foil in AlMn/AlFe compacts shows a yield of 50-75%. This has been confirmed on many occasions both on lab scale and in practice. It implies that these products introduce and form undesired Al_2O_3, which will also show up in the dross. Dr. Langerweger (see ref. 11) reported that, compared to splatter, the AlMn75 compacts generated a three

times higher dross yield. In addition, there is the danger of undissolved phases occurring in some of these products as proper wetting is not secured. The overall loss as a % of carrier input varies from 4 - 24%, depending on type of carrier and the conditions under which they are added.

Conclusion:

Taking all these factors into account, the following table (Table V) summarizes the dissolution rate, coupled with advantages and disadvantages of several Mn and Fe carriers. The calculation of the dissolution rate is also included.
The table clearly shows that both ingot products (AlFe10, AlMn10) and splatter products (AlFe45, AlMn60) are to be preferred. These products also have preference costwise.

Mn carrier	Size of Mn phase content: diameter or thickness mm	Size of Mn phase content: width mm	Density of Mn containing ph. kg/m3	Wettability	Typical dissolution time at 750°C (min)	Danger of undissolved Mn	Nett dross as % of input weight
Mn flakes	1–3	20–50	7.43	average	60	yes	1–10
Mn powder induction	0,500	–	7.43	poor	20–30	yes	1–10
AlMn10 ingot	0,15	–	3.1#	excellent	5	no	<5
AlMn60 splatter	1 *	30–60	4.5	good	9	no	<4
AlMn75 compacts	0,350	–	7.43	average	20	yes	8–10
AlMn75 tablets	0,350	–	7.43	excellent due to flux	15	no	24–26
Mn80 AlloyPack	0,250 µm	–	7.43	excellent due to flux	4	no	22–24
Mn90 AlloyPack	covered with flux					no	12–14

AlMn6 phase
* After addition to liquid Al, very fine particle size due to the shattering effect

Fe carrier	Size of Fe containing phase	Density	Wettability	Typical dissolution time at 750°C (min)	Danger of undissolved Fe	nett dross as % of input weight
AlFe10 ingot	0,15	3,0	excellent	5	no	<4
AlFe45 splatter	1 *	4.0	good	20	no	<4
AlFe75 compacts	0,35	7.86	average	20	yes	7–17
Fe75 flux tablets	0,35	7,86	excellent	20	no	24–26
Fe80 AlloyPack	0,35	7,86	excellent	20	no	22–24

* After addition to liquid Al very fine particle size due to the shattering effect

Table V: Properties that directly determine the rate of dissolution.

Implications for dissolution of other master alloys:

Sr modification:
A newly developed production process for fine phased alloys has been introduced, which enables the manufacturing of ductile highly concentrated alloys. The novel binary fine phased AlSr10 alloy is an example of this development.
As illustrated in Table I, in the case of the AlSr phase a conventional Al-Sr master alloy in rod form is available, dissolving within 1-2 minutes. The novel AlSr10 alloy with very fine intermetallic Al_4Sr phase (5µm. thickness) gives a remarkable performance. Due to its small intermetallic size, the calculated time for dissolution is in the order of seconds (see Table I). In fact the role of Al_4Sr particles in the modification process is eliminated. Modification experiments were carried out on three master alloys by the University of Stockholm, conventional AlSr10 waffle ingot, AlSr3.5 rod and AlSr10 rod, produced via the novel process (see ref. 13). These three alloys, containing different $AlSr_4$ phase sizes in relation to holding time, are plotted in figure 3.

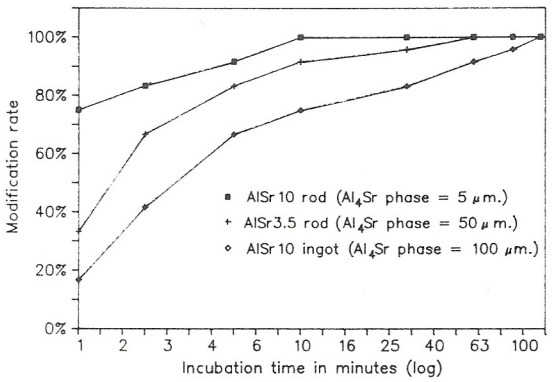

Figure 3: Modification of alloy 356 with 0.015% Sr.

If the basic AlSi alloy contains phosphorus, the modification behaviour will become affected and the following sequence is likely to occur:

1. The dissolution of Al_4Sr particles through the formation of Al_2Si_2Sr. For example:

   $Al_4Sr \longrightarrow Al_2Si_2Sr \longrightarrow (Sr)$ in solution (reaction 1)

2. The neutralization of the modifier by a reaction of Sr and AlP.
   As a result Sr is removed from liquid solution and the modification rating will decrease.
   For example:

   AlP + (Sr) in solution $\longrightarrow$ Al + SrP (reaction 2).

Recent experiments have shown that the P content can be dealt with. The modification rating was determined by adding 0.015-0.02% Sr to AlSi7Mg alloys containing 25 ppm P. The same three master alloys were used.
The outcome of the experiments is depicted in figure 4.

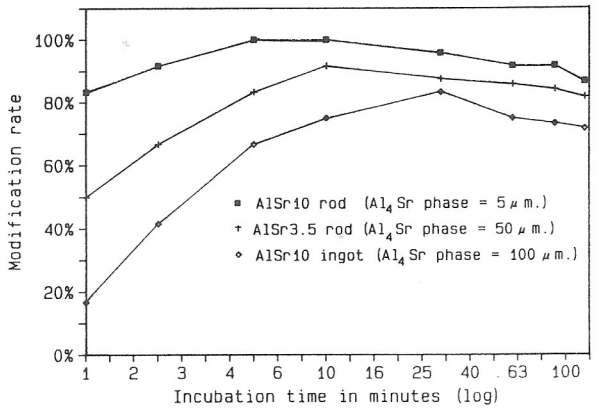

Figure 4: Modification of alloy 356 with 0.022% Sr and 0.0025% P

To explain the observed phenomena, it can be assumed that the rate of reaction 1 is determined by the size of Al_4Sr, whereas the rate of reaction 2 is determined by the quantity of Sr in solution and the level of P.

If a surplus of (Sr) in solution is maintained, there will be enough Sr available for the modification of the eutectic. This is the case when small Al_4Sr is provided in the master alloy. If shortage of (Sr) in solution is obtained, as will be the case with slow-dissolving large Al_4Sr needles, there will never be enough Sr in solution to obtain a full modification. When P is absent, the modification rating is permanent.

Clearly, the new AlSr10 master alloy being produced enables the modification of high P content melts, which can not be achieved with standard AlSr master alloys.

Other master alloys:

As shown in Table I, the rate of dissolution can be calculated and compared to practical experience. The basic know-how provided by the dissolution model, in combination with a production process that yields fine intermetallic phases, offers significant scope for the development of existing and novel master alloy compositions.

Conclusions:

Phase control in AlTiB grain refiner alloys has lead to the development of a robust multi-purpose grain refiner, in which the control of the size of the Al_3Ti and TiB_2 phase has a direct effect on the performance of the master alloy.

Phase control during casting of Aluminium based Mn and Fe carriers yields a splatter product. When added to the melt this product causes a shattering effect, which leads to controlled dissolution time with minimal dross generation.

Phase control in the novel AlSr10 fine phased alloy enables the direct introduction of Sr into Al-Si casting alloys. This offers scope for the introduction of the concept of in-line treatment. The dissolution of Sr in a matter of seconds directly introduces Sr in liquid solution. This provides a fast-acting modification which is maintained, even with a moderate phosphorus content.

Capitalizing on the progress made, a development programme was drafted in which phase control and the production of highly concentrated master alloys are the key interests.

Developments implemented by KBM are subject to the rules of the ISO 9001 standard (see ref. 12).

References:

1. R.J. O'Malley, C.E. Dremann and D. Apelian. J. Metals, February 1979. pp 14-19. Alloying of Molten Aluminium by Manganese Powder Injection.

2. H. d'Hondt. Part I, Proceedings of 26th Annual Conference of Metallurgists of CIM in Canada. August 1987.

3. E. van Erckelens, Ertsbergbau, Einschl. Aufbereitung XX(NFXI). 1923. 11 pp 206-210. Aluminium-Titan Legierungen und der Einfluss des Titans auf Aluminium.

4. M. Vader and J. Noordegraaf. Light Metals 1989. Edited by P.G. Cambell. TMS 1989. pp 937-941. The New Approach to Grain Refining.

5. M. Vader and J. Noordegraaf. Light Metals 1990. The Effectiveness of a Grain Refiner Reinforced by a Built-In Energy Content. TMS 1990. pp 851-857.

6. L. Bäckerud and S. Yidong. Grain refining Mechanisms in Aluminium as a Result of Additions of Titanium and low Boron. Part I: Nucleation and growth below the bulk liquidus temperature.

7. L. Bäckerud, P. Gustafson and M. Johnsson. Grain Refining mechanisms in Aluminium as a Result of Additions of Titanium and low Boron. Part II: Nucleation and growth above the bulk liquidus temperature.

8. N.J. Finch. Met. Trans 3 (1972) pp 2709-2711. The Metal Solubilities of Titanium and Boron in Pure Aluminium.

9. J.L. Murray, Met Trans. 19a (1988) pp 243-247.

10. M. Vader and J. Noordegraaf. 8th International Leichmetalltagung Leoben, Austria 21st-25th June 1987. pp 464-467 Interrelations Between Aluminium Grain Refining by Means of Al-Ti-B Alloys and the Number of Growth Centres.

11. J. Langerweger. Schweizer Aluminium Rondschau 32 (1982) 2 pp 51-57. Legierungstechnik und Schmelzvorbehandlung mit Vorlegierungen in der Aluminiumindustrie.

12. J. Noordegraaf and M. Vader. Aluminium 1990, October. Quality Assurance in Master Alloy Production.

13. G. Chai and L. Bäckerud. Factors Affecting Modification of Al-Si Alloys After Additions of Sr. (To be published).

Dissolution time in sec.: $t = \frac{\rho \, d_o \, F_x(ß)}{60 \, k \, (C_s - C_i)}$

ρ = density, kg/m^3
d_o = initial diameter or thickness, m
F_x = Function dependent on ß and mass fraction x dissolved. In this case only F_{100} and F_{95} are considered, see also table and graph.
x = % of mass fraction dissolved..
k = average mass transfer co-efficient which is taken as $3\ 10^{-5}$ m/s (see O'Malley et al, ref 1 and Paret and d'Hondt, ref 2)

$ß = \frac{C_f - C_i}{C_s - C_i}$

C_f = final concentration
C_i = initial concentration
C_s = saturation concentration (liquid solubility) as determined by the equilibrium phase diagram all in mass %

$F(x,ß) = F_x(ß)$ = dissolution function (dependent on ß and x)

(See also Table and graph)

Example: $F_{95} = \exp(1.326ß + 0.251)$, corr. = 0,991

Table

ß	F_{100}	F_{95}
0.01	2.5	1.4
0.1	2.65	1.5
0.2	3.1	1.7
0.3	3.35	1.8
0.4	3.9	2.1
0.5	4.45	2.4
0.6	----	2.7
0.7	----	3.1
0.8	----	3.9
0.9	----	4.6

Graph

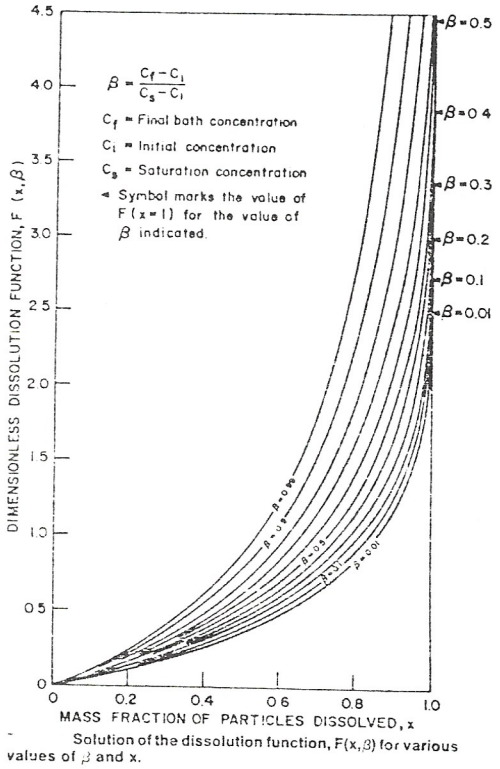

Solution of the dissolution function, F(x,β) for various values of β and x.

(Reproduced from Ref. 1.)

Appendix 1: Model for calculation of the dissolution rate.